ORIGINAL PAPER

Spectral Properties of Y-Shaped Donor-Acceptor Push-Pull Imidazole-based Fluorophores: Comparison between Solution and Polymer Matrices

Martin Danko · Filip Bureš · Jiří Kulhánek · Pavol Hrdlovič

Abstract The spectral properties of a novel type of Y-shaped fluorophores consisting of an imidazole ring end-capped with two electron-donating N,N-dimethylaminophenyl groups at positions C4 and C5 and one electron-withdrawing cyano group on the imidazole moiety at position C2 were examined. The π-linker separating the 4,5-bis[4-(N,N-dimethylamino) phenyl]-1H-imidazole donor moiety and the cyano group comprises 1,4-phenylene (**1**), (E)-phenylethenyl (**2**), (E)-phenyl-buta-1,3-dienyl (**3**), biphenyl (**4**), (E)-phenylethenylphenyl (**5**) and phenylethynylphenyl (**6**) conjugated paths. The absorption and fluorescence spectra were obtained in toluene, dichloromethane, acetonitrile and methanol and in polymer matrices such as polystyrene (PS), poly(methyl methacrylate) (PMMA) and poly(vinylchloride) (PVC). The most intense absorption bands of fluorophores **1–6** were observed within the range of 283 to 330 nm. Less intense but longer-wavelength absorption bands designated as charge-transfer bands were observed at approximately 380–430 nm depending on the medium. The fluorophores exhibited strong fluorescence in the visible region with a Stokes shift of approximately 4300–5800 cm^{-1} in non-polar toluene and polystyrene, whereas very low intensity of fluorescence was observed with a Stokes shift in the 6500–7800 cm^{-1} region in polar methanol and acetonitrile. The large Stokes shift indicates a large difference in the spatial arrangement of the chromophore in the absorbing and emitting states. A relatively intense fluorescence (quantum yields of 0.12–0.69) was observed only for derivative **1** in all media except methanol. The fluorophores doped in matrices yielded more intense fluorescence compared with the fluorescence in liquid media. The use of solid polymer matrices lowers the probability of forming non-emissive excited states. The fluorescence lifetimes were short (1–4 ns) for all of the fluorophores in solvents and in polymer matrices.

Keywords Fluorescence · Push-pull System · π-linker · Imidazole · Polymer matrices

M. Danko (✉)
Polymer Institute, Center of Excellence GLYCOMED,
Department of Synthesis and Characterization of Polymers,
Slovak Academy of Sciences,
Dúbravská cesta 9,
845 41 Bratislava, Slovakia
e-mail: upoldan@savba.sk

F. Bureš · J. Kulhánek
Institute of Organic Chemistry and Technology,
Faculty of Chemical Technology, University of Pardubice,
Studentská 573,
53210 Pardubice, Czech Republic

P. Hrdlovič
Polymer Institute, Slovak Academy of Sciences,
Dúbravská cesta 9,
845 41 Bratislava, Slovakia
e-mail: upolhrdl@savba.sk

Introduction

Photonics, which involves the generation, emission, transmission and modulation of light as well as its signal processing, switching, detection and sensing, is an intensively developing branch of science. Simultaneously, photonics is a basis for new technologies that exploit the capability of photons to carry information and energy [1–4]. To achieve this goal, new organic materials with properties such as large nonlinear susceptibilities, fast responses and easy preparation and handling should be developed. The organic π-conjugated compounds having both electron donor (D) and acceptor (A) parts exhibit interesting optical and spectral properties due to intramolecular charge transfer (ICT) from the donor to the acceptor and, therefore, have attracted considerable attention [5]. The

electron donors and acceptors in such molecules are connected by a π-conjugated system of single and multiple bonds. A typical arrangement of these chromophores is a linear D-π-A system in which D is a strong electron-donating group (e.g., NH₂, NR₂ or OR) and A is a strong electron-withdrawing group (e.g., an NO₂ or CN group) [6–11].

We and others have reported several push-pull systems with electron donors or acceptors attached to various π-conjugated linkers to achieve better tuning of spectral properties, solvent effects, polarizabilities and partial or full charge separation [12–23]. These organic molecules exhibit various degrees of flexibility in the ground and excited states that might be correlated with the relevant radiation and radiation-less processes. ICT chromophores and their unique properties attract considerable attention in both photochemistry and photobiology because of their high susceptibility to some environmental parameters, such as micro-viscosity and micro-polarity. During the last three decades, D-π-A systems were intensively studied as tunable materials for non-linear optics (NLO) [8], optical data storage devices [24], organic light emitting diodes (OLED) [25], organic–inorganic hybrid materials [26], functional polymers [27] and dendrimers [28].

Recently, we reported the spectral properties of push-pull systems featuring imidazole-4,5-dicarbonitrile as an electron acceptor moiety and an N,N-dimethylamino group as an electron donor connected by various types of π-linkers (Scheme 1), which were studied both in solution and in polymer matrices [17, 29]. These D-π-A push-pull systems exhibited fluorescence in non-polar solvents and common polymer matrices. In polar solvents such as methanol and acetonitrile, the fluorescence was completely quenched. In the present paper, we report the spectral characteristics of six new molecules representing a typical push-pull system (Scheme 1, 1–6) featuring 4,5-bis[4-(N,N-dimethylamino)phenyl]-1H-imidazole as a donor moiety. This imidazole structural unit is linked to the cyano acceptor group by a π-conjugated system consisting of 1,4-phenylene (1), (E)-phenylethenyl (2), (E)-phenylbuta-1,3-dienyl (3), biphenyl

(4), (E)-phenylethenylphenyl (5) and phenylethynylphenyl (6). Whereas the first series of compounds, based on the imidazole-4,5-dicarbonitrile, possesses two acceptors and one donor at the imidazole C4/C5 and C2 positions [29], respectively, the new series of chromophores 1–6 represents structurally reversed analogs. These compounds feature two donors at the imidazole positions C4/C5 and one acceptor at the C2 position connected by the aforementioned π-linkers. The primary aim of this paper is to characterize these push-pull systems with a higher number of electron donors in solution as well as in polymer matrices and to compare their properties with those of the previously studied imidazole-4,5-dicarbonitrile-derived chromophores. Secondly, we will attempt to understand the correlation between the chromophore structure and its spectral properties to develop D-π-A push-pull materials with tunable properties and to extend the potential applications of these materials in photonics.

Experimental

The molecular structures of the investigated fluorophores 1–6 are given in Scheme 1. Their detailed syntheses have been published elsewhere [21].

Anthracene was zonnally refined (Lachema n.e., Brno, CR). Methanol (MeOH, Scharlau Chemie s.a., Sentmenat, Spain), dichloromethane (CH₂Cl₂, Sigma-Aldrich), toluene (Sigma-Aldrich), chloroform (CHCl₃, Scharlau Chemie s.a., Sentmenat, Spain), tetrahydrofuran (Scharlau Chemie s.a., Sentmenat, Spain) and acetonitrile (AcCN, Merck, Bratislava, SR) were of spectroscopy grade and were used without further purification.

Polymer films doped with the fluorophores (1–6) at a concentration of 0.002 mol kg^{-1} were prepared by casting from solution. Films of polystyrene (PS) (Chemische Werke Huels, F.R.G.) and poly(methyl methacrylate) (PMMA) (Diacon, ICI, England) were prepared by casting 1 ml of the chloroform solution of polymer (5 g/100 ml) containing the
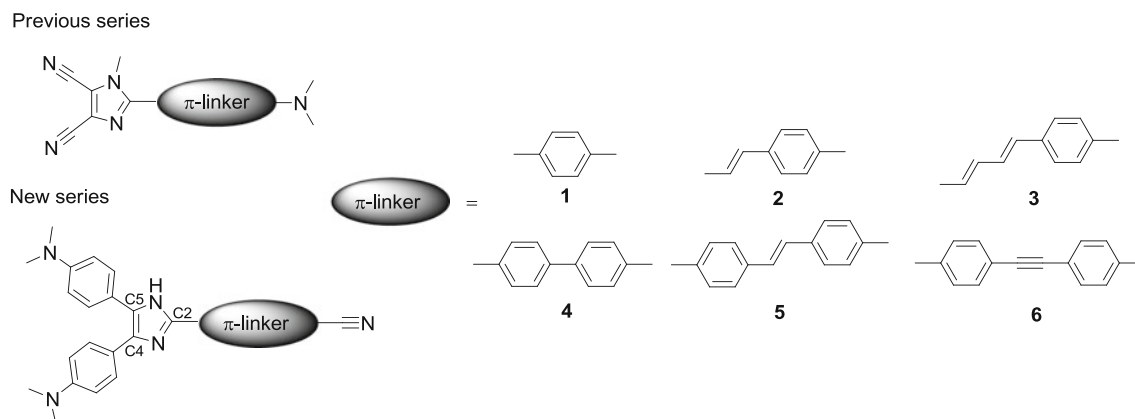
Scheme 1 Molecular structures of the investigated Y-shaped imidazole derivatives 1–6

desired amount of probe on a glass plate (28×35 mm). The solvent was slowly evaporated. Films of poly(vinylchloride) (PVC) (Neralit, Spolana Neratovice s.e., CR) were prepared in a similar manner by casting from a tetrahydrofuran solution. The UV–VIS absorption spectra were obtained using an UV 1650PC spectrometer (Shimadzu, Japan). The emission spectra were recorded using a RF-5301PC spectrofluorophotometer (Shimadzu, Japan). The fluorescence of the solutions was measured in 1 cm cuvette in a right-angle arrangement. The fluorescence of the polymer films was measured in a front-face arrangement on the solid sample holder. The quantum yields were determined relative to anthracene. The quantum yields of anthracene fluorescence in different media, which were determined by comparing the fluorescence of anthracene in cyclohexane ($\Phi=0.25$ [30]) to that in the media used in this study, were determined to be 0.20 in methanol and acetonitrile, 0.16 in toluene and 0.11 in dichloromethane. In the polymer matrices, the quantum yields were assumed to be 0.20 in PMMA, 0.16 in PS and 0.11 in PVC. The quantum yields in the solutions and films were corrected to different absorptions at the excitation wavelength [31]. The fluorescence spectra were obtained by exciting into the maximum of the longest wavelength absorption band.

Experimental setup for detection of fluorescence lifetimes in solvents was based on time-correlated single-photon counting (TCSPC) setup, analogical to the one described in details in [32] (all components from Becker&Hickl GmbH, Berlin, Germany). Shortly, the sample in quartz cuvette was excited by 375 nm picosecond diode laser with output power ~1 mW, pulse widths typically around 50 ps and frequency rate (20 MHz). The emitted fluorescence was spectrally separated from the laser excitation using 395 nm dichroic filter. A polarizer in magic-angle orientation was fitted in front of the detection system to avoid distortions of decay kinetics due to depolarization effects. The emission was measured by a 16-channel multi-anode photomultiplier array attached to the 160 mm spectrograph (PML-SPEC). The PML detector was running in the photon-counting regime and fed the TCSPC interface card SPC-830. Fluorescence decays were measured with 50 ns time-base sampled by 1024 temporal channels. The fluorescence lifetime measurements in solid polymer films were performed using a LIF 200 (Lasertechnik Ltd., Berlin, F.R.G.), which operates as a stroboscope. The excitation source was a nitrogen laser emitting at 337 nm, and the emission was selected using a cut-off filter. The output signal of the boxcar integrator was digitized and transferred to the PC using a home-made program. The fluorescence decay curves were evaluated using a simple phase plane method [33] implemented in J. Snyder's program based on a previous work [34]. The standard deviation $G^{1/2} = \Sigma\left(\left(I_{exp} - I_{calc}\right)^2/n\right)^{1/2}$, where I_{exp} and I_{calc} are the intensities of the experimental and calculated emissions, respectively, was used to judge whether the decay was mono-exponential. The decay curve was assumed to be mono-exponential when $G^{1/2}$ was less than 5 %. Alternatively, the fitting of the fluorescence decay curves for a bi-exponential decay model was performed using the adapted FluoFit MatLab package [35].

Results and Discussion

Absorption Characteristics in Solution

In general, the spectral properties of compounds with push-pull interactions such as **1–6** (Scheme 1) are determined by the ICT extent. The investigated push-pull molecules **1–6** differ in the type of π-linker separating the 4,5-bis[4-(N,N-dimethylamino)phenyl]-1H-imidazole donor unit and the cyano acceptor group. Molecules **1–6** can be further subdivided into two groups according to the type of connection between the imidazole and the π-linker. Whereas the first group represents molecules with the 1,4-phenylene subunit connected directly to the imidazole at the C2 position (**1, 4–6**, Scheme 1), the second group is composed of molecules with one or two additional ethylene bridges planarizing the entire π-system (**2, 3**, Scheme 1).

The most intense absorption bands of probes **1–6** lie within the interval 283–330 nm in all of the investigated media. In addition to this absorption band, well distinguished ICT bands with λ_{max} in the range of 375 to 450 nm were observed. (Table 1, Figs. 1, 2 and 3). It is obvious that the position and shape of the entire spectrum depend primarily on the length and planarity of the π-linker. The most bathochromically shifted bands relative to the parent probe **1** were observed for probes **2** and **3** due to the ethylene/buta-1,3-diene bridges. The absorption bands of **1–6** were slightly hypsochromically shifted in order from non-polar toluene and dichloromethane to polar protic MeOH and aprotic AcCN (Table 1). The influence of the π-linker length on the position of the longest-wavelength band was demonstrated using probes **2** and **3**. Compared with probe **1**, these chromophores possess λ_{max} values that are bathochromically shifted by up to 50 nm. The replacement of a non-polar medium with a polar medium caused a hypsochromic shift within the range of 10 to 19 nm, according to the polymer matrix used (Fig. 2).

Extension of the parent 1,4-phenylene moiety, such as that in **1**, by another 1,4-phenylene moiety (**4**) resulted in a hypsochromic shift as a direct consequence of the biphenyl linker twist. Although chromophore **4** possesses a longer π-linker than **1**, the non-planar biphenyl arrangement hinders an efficient D-A interaction; therefore, the spectrum exhibits a slight hypsochromic shift. This observation was discussed in our earlier works [19, 23]. Conversely, π-linkers such as (E)-phenylethenylphenyl and phenylethynylphenyl in **5** and

Table 1 Absorption characteristics of probes **1–6** in different solvents and polymer matrices

Probe[a]/medium[b]	1 λ_A[c] nm (log ε)	2 λ_A[c] nm (log ε)	3 λ_A[c] nm (log ε)	4 λ_A[c] nm (log ε)	5 λ_A[c] nm (log ε)	6 λ_A[c] nm (log ε)
toluene	315	313	327	295	322	316
	396 (4.45)	428 (4.20)	447 (4.18)	394 (4.29)	415 (4.20)	408 (4.47)
CH$_2$Cl$_2$	316	313	326	276	322	315
	396 (4.41)	422 (4.43)	442 (4.59)	388 (4.33)	411 (4.37)	403 (4.50)
AcCN	318	307	324	284	319	312
	388 (4.50)	416 (4.35)	428 (4.39)	379 (4.43)	404 (4.42)	396 (4.44)
MeOH	309	307	321	283	318	309
	385 (4.33)	416 (4.50)	429 (4.28)	375 (4.49)	398 (4.42)	390 (4.44)
PS	315	314	330	292	327	318
	398 (4.12)	433 (4.20)	450 (4.12)	399 (4.21)	425 (4.19)	412 (4.18)
PMMA	314	311	327	295	326	316
	394 (4.42)	425 (4.27)	441 (4.25)	390 (4.41)	410 (4.34)	405 (4.41)
PVC	319	319	329	307	331	323
	389 (4.30)	427 (4.23)	437 (4.20)	385 (4.37)	411 (4.39)	402 (4.33)

[a] Structure of probes **1–6** is according to Scheme 1

[b] Medium: CH$_2$Cl$_2$—dichloromethane; AcCN—acetonitrile; MeOH—methanol; PS—polystyrene; PMMA—poly(methylmethacrylate); PVC—poly(vinylchloride)

[c] Maxima in absorption spectrum. Numbers in parentheses indicate the molar decadic extinction coefficient calculated from ε, which is in L mol^{-1} cm^{-1}

6 caused a bathochromic shift of the ICT band as a result of the π-conjugated path elongation and partial planarization.

Absorption Characteristics in Polymer Matrices

The absorption spectra of probes **1–6** are similar in all of the polymer matrices used, and they resemble those measured in dichloromethane in this study or in ref. [21]. Distinguished absorption bands were generally observed in the UV region, with the maximum ranging from 292 to 331 nm. The bathochromically shifted bands, whose position depends on the structure of the π-linker, were well resolved and range from 385 to 450 nm. The largest bathochromic shift of the ICT band was observed for **3** in PS (λ_{max}=450 nm) (Fig. 2). In general, the absorption bands were bathochromically shifted in less polar PS than in the PMMA and PVC matrices. All of the above deduced structure–property relationships affecting the spectral properties such as the length and planarity of the used π-linker were applicable in all of the investigated liquids and
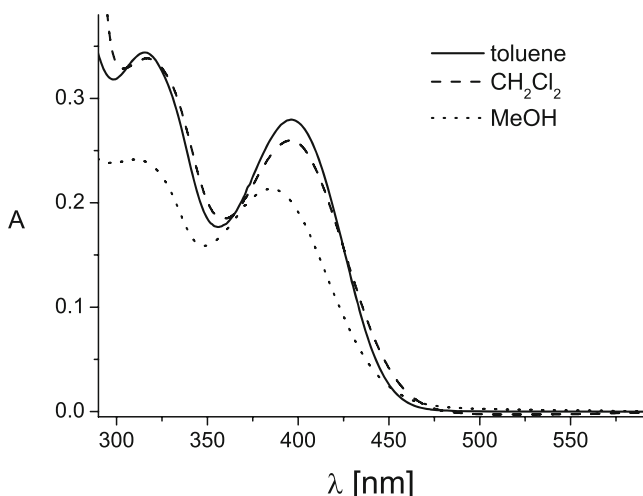

Fig. 1 Absorption spectra of chromophore **1** measured in toluene, dichloromethane and methanol at a concentration of 10^{-5} mol L^{-1}
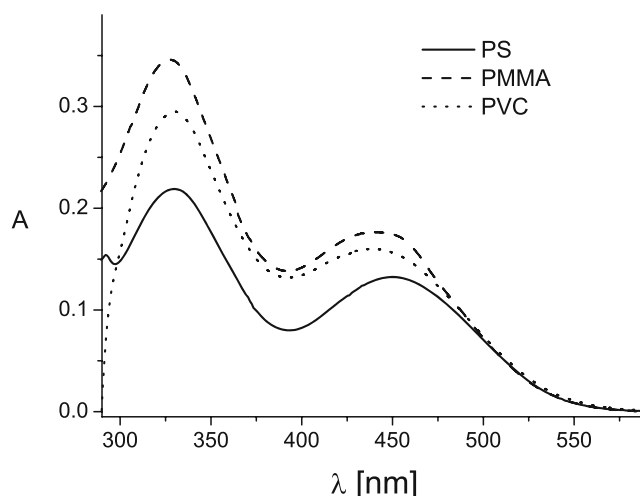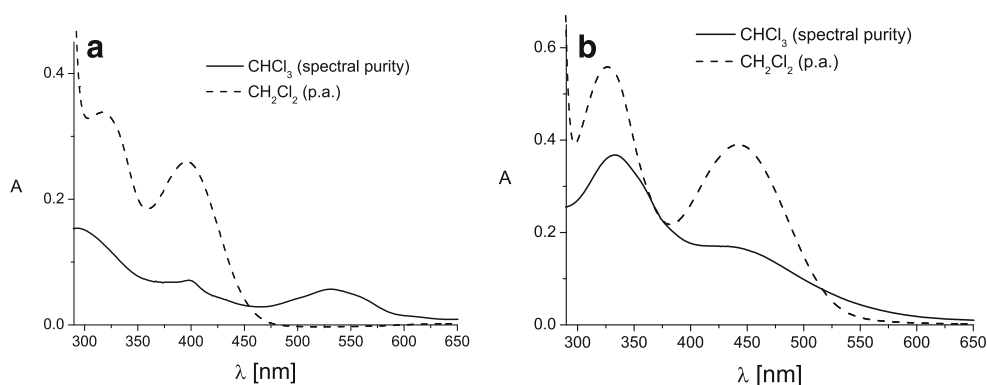

Fig. 2 Absorption spectra of chromophore **3** measured in PS, PMMA and PVC polymer matrices at a concentration of 0.002 mol kg^{-1}

Fig. 3 Comparison of the absorption spectra of chromophores (a) 1 and (b) 3 measured in dichloromethane and chloroform at a concentration of 10^{-5} mol L^{-1}. The chloroform solvent was not purified before the measurements

the solid media. These relationships play the most important role in non-polar media.

Notably, the investigated chromophores are very sensitive to the residual acidity potentially present in some solvents. The residual HCl, especially in chloroform, led to the protonation of the terminal *N,N*-dimethylamino donor groups and the formation of an A-π-A^{+} system instead of an A-π-D system with diminished ICT. This protonation resulted in the disappearance of the ICT band (Fig. 3). Such protonation/neutralization sensitivity of push-pull systems can be used to generate pH-triggered switches [23].

Probes **1–6** were relatively stable when doped into polymer matrices. In the cases of PS and PMMA, the absorption spectra did not change for weeks if the complexes were stored in the dark. A gradual formation of HCl in the PVC matrix led to a slow decrease of the ICT band, as observed in the case of chloroform (Fig. 4). A complete disappearance of the ICT band was observed after approximately eight weeks.

The spectral data for reversal push-pull molecules with *N,N*-dimethylaminophenyl donor and imidazole-4,5-dicarbonitrile acceptor moieties separated by similar π-linkers (see Scheme 1)
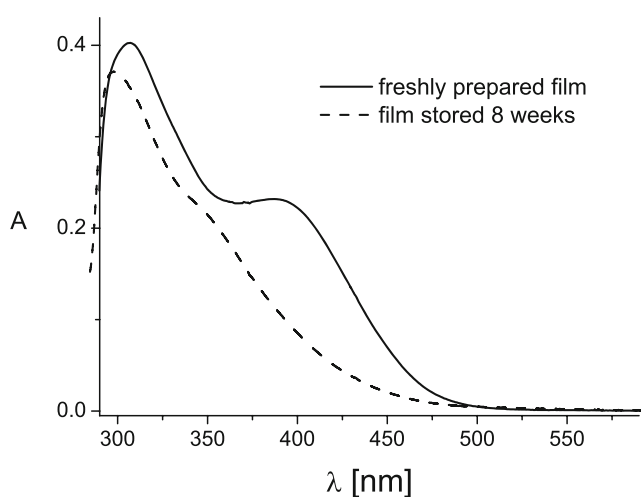
Fig. 4 Absorption spectra of chromophore 4 measured in a PVC matrix at a concentration of 0.002 mol kg^{-1}. The spectra were measured when the samples were fresh and after they had been stored in the dark for approximately 8 weeks

resemble those for chromophores **1–6** [29]. Upon transferring from non-polar to polar media, all of these derivatives exhibited hypsochromically shifted ICT absorption bands, and the most hypsochromically shifted band was observed in polar MeOH. However, the longest-wavelength absorption maxima of the previous series [29] (similar π-linkers as those of **1, 4–6**) do not exceed 400 nm. This result implies that the imidazole chromophore arrangement with two donors and one acceptor without N1-alkylation, as observed in **1–6**, assures better ground state D-A conjugation.

Emission Characteristics in Solution

The fluorescence spectra of probes **1–6** in liquid media were obtained with an excitation wavelength corresponding to the position of the ICT bands. The fluorescence intensity and vibrational structure of the spectra of particular chromophores depend on the solvent used. All of the emission parameters of probes **1–6** are listed in Table 2. In non-polar toluene and dichloromethane, a wide non-structured band in the range from 500 to 600 nm was observed (Fig. 5a). In polar media, some vibrational emission structure in the form of a bathochromically shifted shoulder related to the main emission band was observed for probes **2, 3** and **4** (Fig. 5b). In all liquid media, the positions of the emission maxima depend on the length and planarity of the π-linker between the donor and acceptor, similar to that observed in the absorption spectra. The bathochromic shift of the emission maxima increased in the order of **3, 2, 5, 6** and **4**. Basic probe **1** exhibited an emission at the shortest wavelength in all media. The Stokes shifts express the nature of the excited state and its stabilization in a particular environment. The lowest values of the Stokes shifts were observed in non-polar toluene for all probes ranging from 4300 cm^{-1} for **3** to 5800 cm^{-1} for **4**. The observed Stokes shifts in polar solvents were within the range of 6500 cm^{-1} for **5** in AcCN to 7800 cm^{-1} for **1** in MeOH. Moreover, the Stokes shifts of **2, 3** and **4** were spread over a wide range of wavelengths as a consequence of the observed dual (shoulders) and low-intensity fluorescence. For example, the highest Stokes shift was observed for **4** in dichloromethane (8137 cm^{-1}), but two fluorescence bands were observed in polar AcCN with

Table 2 Emission parameters of the investigated probes **1**–**6** in different solvents

Probe[a]/Parameter	Medium[b]	λ_F [c] nm	Φ_F [d]	ν [e] cm^{-1}	τ_F [f] ns	$k_{F\text{-}cal}$ [g] $\times 10^8$ s^{-1}	$\tau_{F\text{-}cal}$ [h] ns
1	toluene	486	0.37	4676	2.9	2.82	1.0
	CH$_2$Cl$_2$	542	0.14	6802	3.7	2.57	0.54
	AcCN	550	0.12	7591	–	3.16	0.4
	MeOH	551	0.02	7825	–	3.14	0.08
2	toluene	536	0.25	4708	3.2	1.58	2.0
	CH$_2$Cl$_2$	586	0.03	6632	2.2	2.69	0.1
	AcCN	600, 631sh	0.01	7372 (8191)	–	2.24	0.05
	MeOH	588	0.003	7032	–	3.16	0.01
3	toluene	555	0.13	4353	2.8	1.51	0.9
	CH$_2$Cl$_2$	601	0.01	5985	1.6	3.89	0.03
	AcCN	606, 632	0.002	6863 (7542)	–	2.45	0.009
	MeOH	599	0.001	6616	–	1.91	0.005
4	toluene	511	0.29	5811	2.9	1.91	1.0
	CH$_2$Cl$_2$	567	0.02	8137	1.6	2.14	0.04
	AcCN	432, 591	0.001	3237 (9465)	–	2.69	0.005
	MeOH	428, 549	0.002	3302 (8451)	–	3.09	0.006
5	toluene	540	0.15	5578	3.2	1.58	0.94
	CH$_2$Cl$_2$	540	0.005	5812	1.0	2.34	0.022
	AcCN	549	0.002	6538	–	2.63	0.006
	MeOH	553	0.001	7042	–	2.63	0.002
6	toluene	522	0.23	5353	2.8	2.95	0.78
	CH$_2$Cl$_2$	565	0.001	7115	–	3.16	0.003
	AcCN	wide 530	0.002	–	–	2.75	0.005
	MeOH	536	–	6984	–	2.75	0.001

[a] Structure of probes **1**–**6** is according to Scheme 1

[b] Medium: CH$_2$Cl$_2$—dichloromethane; AcCN—acetonitrile; MeOH—methanol

[c] Maxima in emission spectrum ("sh" means shoulder). Excitation wavelength was set to the absorption maxima according to Table 1

[d] Quantum yield of fluorescence based on anthracene

[e] Stokes shift

[f] Lifetime of fluorescence. Decay was fitted to mono-exponential function

[g] Calculated rate of fluorescence based on Eq. 1

[h] Calculated lifetime based on Eq. 2

calculated Stokes shifts of 3237 cm^{-1} and 9465 cm^{-1} (Fig. 5b). This result can be rationalized as a consequence of the stabilization of two forms of the molecule structure. The large Stokes shifts in polar solvents (Table 2) that were calculated using the wavelength of the emission band shoulders can be explained as a result of the stabilization of the highly polar excited state related to ICT formation. ICT is easily formed through planar and conjugated linkers, which is the case for probes **2** and **3**. Conversely, considering the possible partial rotation within the biphenyl moiety in **4**, such conjugation should be partially disrupted. Moreover, the probes exhibited low fluorescence intensity in polar solvents; thus, a more detailed study using time-correlated fluorescence measurements was not performed.

The observed fluorescence intensities expressed as absolute quantum yields (Φ_F) were relatively low in all media. In comparison with the fluorescence of previously developed imidazole-derived probes (Scheme 1, [29]), the Φ_F values of the probes in this study were lower in particular solvents. From a series of investigated probes, probe **1** exhibited the most intense fluorescence in all media. The most intense fluorescence was observed in non-polar toluene, and the calculated quantum yields were in the range from 0.13 for chromophore **3** to 0.37 for chromophore **1**. In contrast, the fluorescence in polar protic methanol was 1 to 3 orders of magnitude less intense than that in toluene. Generally, the fluorescence quantum yields are strongly dependent on the environment both in solution and in polymer matrices. A critical examination of Table 2 reveals that in solvents of low polarity (limited to toluene because of solubility), the quantum yield was higher (in the range 0.1–0.4) than in solvents of high polarity. Upon moving to solvents of a
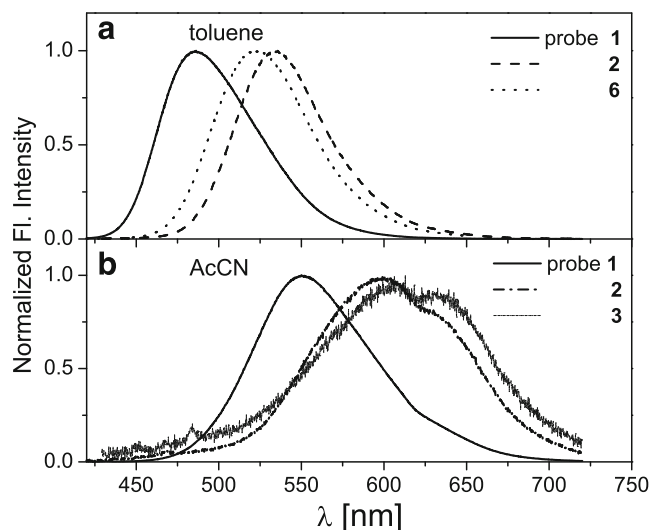
Fig. 5 Normalized emission spectra of probes (**a**) **1**, **2** and **6** in a toluene solution and (**b**) **1**, **2** and **3** in an AcCN solution measured at a concentration of 10^{-5} mol L^{-1}. The excitation wavelengths were set at 396 (**a**) and 388 (**b**) nm for **1**, 428 (**a**) and 416 (**b**) nm for **2**, 428 (**b**) nm for **3**, and 408 (**a**) nm for **6**

higher polarity (dichloromethane, AcCN, MeOH), a drastic decrease in Φ_F was observed in all probes under investigation.

The solvent effects of polar solvents might be related to the non-emissive excited state featuring strong ICT from the electron-donating 4,5-bis[4-(*N,N*-dimethylamino)phenyl]-1*H*-imidazole moiety to the electron-accepting arylcarbonitrile unit at the C2 position. This transition state observed at 375–450 nm in the absorption spectra should be stabilized by polar aprotic solvents and stabilized even more efficiently by protic solvents, which should promote radiationless decay [36, 37]. To ascertain additional details about this interaction, the fluorescence quenching with polar solvents and that with known singlet state quenchers such as an N-oxyl radical (1-oxo-2,2,6,6-tetramethyl-4-hydroxypiperidine, TEMPOL) were compared. The quenching experiments were performed in dichloromethane solutions of **1** and **5** (π-linker connected to imidazole at position C2 via the 1,4-phenylene subunit) as well as for **2** (π-linker connected to imidazole at position C2 via the ethenyl subunit). The quenching experiments using polar solvents were performed with a relatively high concentration of the quencher (polar solvent molecule) within the concentration range from 10^{-1} to 10^{1} mol L^{-1} (0.24–9.6 mol L^{-1} for MeOH and 0.19–7.6 mol L^{-1} for AcCN). This type of quenching was compared with the quenching of a typical singlet quencher such as TEMPOL in the concentration range of 0.001–0.01 mol L^{-1}. No measurable quenching was observed at lower concentrations for this quencher. The dependencies of the fluorescence intensity on the concentration of both polar quenchers for **1** obeyed linear Stern-Volmer relationships (Fig. 6). Particular quenching constants for all of the probes are listed in Table 3. The extent of quenching was higher for MeOH than for AcCN. In fact,

quenching with AcCN was negligible. This difference has also been discussed in previous work related to imidazole-based probes with similar linkers between the donor and acceptor [29]. More effective quenching by MeOH was concluded to be a consequence of the higher concentration of the quencher in the vicinity of the excited probe due to the possibility of hydrogen bonding. However, a completely different quenching mechanism and a slightly lower extent of quenching were observed for probes in this study relative to those investigated earlier.

The quenching of **2** and **5** did not perfectly obey a linear relationship. The quenching of **2** was linear only under the assumption that the first points of both quenching solvent dependencies were omitted. With these approximations, the quenching was similar for both methanol and acetonitrile. The quenching rate constants were slightly higher (0.93×10^{10} and 0.81×10^{10} L mol^{-1} s^{-1} in MeOH and AcCN, respectively) for **2** than those for **1** quenched by methanol (0.70×10^{10}) (Table 3, Fig. 7). The decrease of the fluorescence intensity can be correlated with the increase in the ICT absorption band measured for samples in the same concentration range of quencher. This correlation was clearly visible for the **2**/CH$_2$Cl$_2$/MeOH system (Fig. 7, bottom) but relatively ambiguous for the **2**/CH$_2$Cl$_2$/AcCN system and other investigated samples.

Conversely, the quenching of probe **5** by polar solvents was relatively negligible; the k_q values were nearly 10 times lower and loaded with a high error (very low correlation coefficients of linear fitting). The dependency for methanol quenching was clearly not linear, and the quenching rate constant was calculated only approximately using a Stern-Volmer-like expression (Fig. 8). This quenching was also accompanied by a
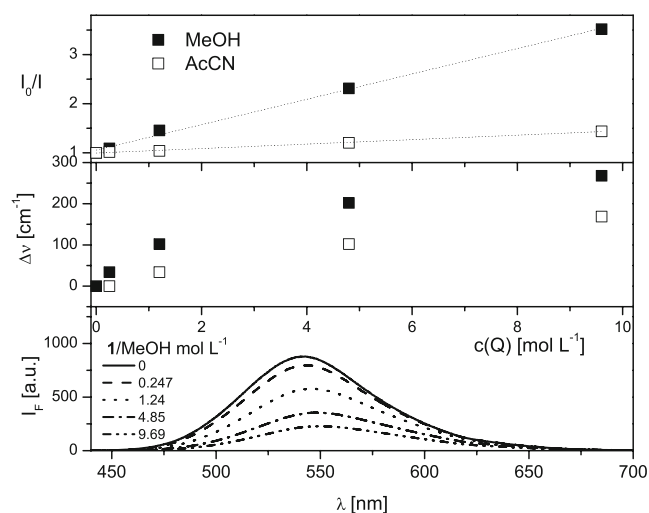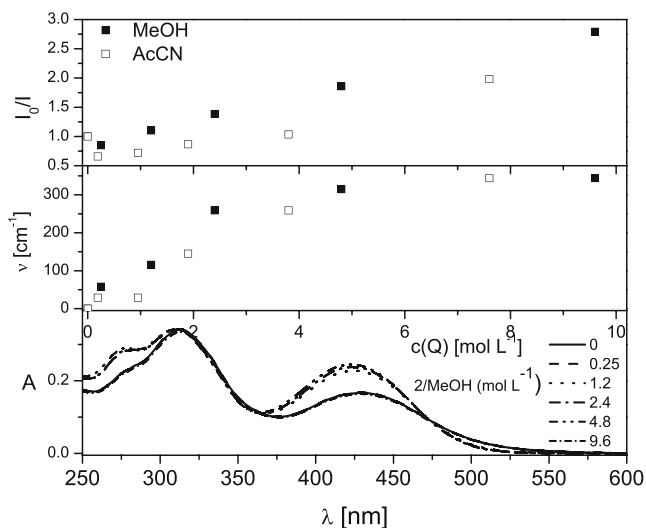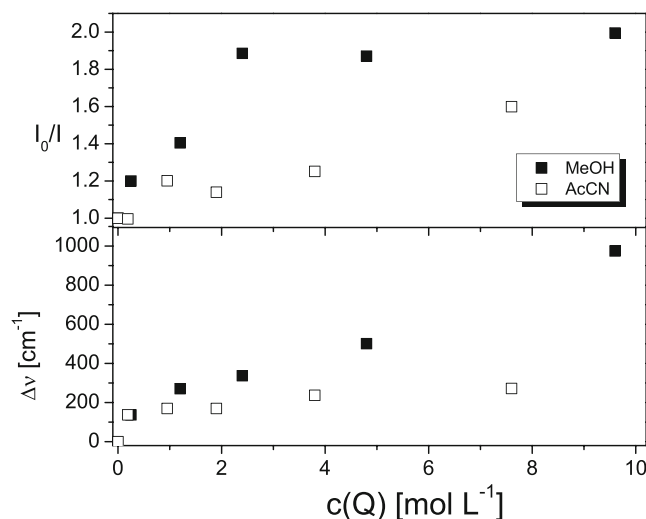

Fig. 6 The dependencies of the fluorescence intensity (integral under the curve) and the shift of the emission maxima of probe **1** measured in CH$_2$Cl$_2$ at a concentration of 10^{-5} mol L^{-1} with the addition of polar quenchers. The excitation wavelength was set at 396 nm. The lines represent linear fits of the experimental points from the Stern-Volmer equation with the parameters listed in Table 4

Table 3 Fluorescence quenching of fluorophores **1**, **2** and **5** in dichloromethane by polar solvents

Probe[a]	Quencher	K_{SV}[b] L mol^{-1}	A[c]	r[d]	τ[e] ns	k_q 10^{10f} L mol^{-1} s^{-1}
1B	MeOH	0.258	1.056	0.9963	3.7	0.70
	AcCN	0.045	0.995	0.9961		0.12
2B	MeOH	0.205	0.851	0.9967	2.2	0.93
	AcCN	0.179	0.537	0.9446		0.81
5B	MeOH	0.092^g	1.28	0.5811	0.98	0.09
	AcCN	0.074	1.02	0.9128		0.07

[a] See Scheme 1 for the sample structures

[b] Stern-Volmer constant

[c] Abscissa on the y-axes

[d] Correlation coefficient

[e] Lifetime in CH_2Cl_2 from Table 2

[f] Diffusion-controlled bimolecular quenching rate constant calculated as K_{SV}/τ

[g] Stern-Volmer-like dependency

bathochromic shift of the emission maxima. The dependence of this shift on the same quencher concentration range exhibited a slightly different shape. In contrast, the shift of the maxima was correlated with the gradual addition of the polar quencher to the dichloromethane solution because $\lambda_F = 542$ nm in pure dichloromethane and $\lambda_F = 551$ nm in pure methanol for probe **1** (Fig. 6). The most visible influence on the position of the emission maxima was observed for **5** quenched by methanol (~900 cm^{-1}). The value of this shift was similar to the difference between the position of the emission maxima in dichloromethane and methanol (960 cm^{-1}).

Fig. 7 The dependencies of the fluorescence intensity (integral under the curve), the shift of the emission maxima and the absorption spectra of probe **2** measured in CH_2Cl_2 at a concentration of 10^{-5} mol L^{-1} with the addition of polar quenchers. The excitation wavelength was set at 422 nm

Fig. 8 The dependencies of the fluorescence intensity (integral under the curve) and the shift of the emission maxima of probe **5** measured in CH_2Cl_2 at a concentration of 10^{-5} mol L^{-1} with the addition of polar quenchers. The excitation wavelength was set at 411 nm

Surprisingly, almost no fluorescence quenching was observed for any of the probes when TEMPOL was used as a quencher in the concentration range from 10^{-3} to 10^{-1} mol L^{-1}. In a previous study [29], TEMPOL was a very efficient quencher of the singlet states of probes with two electron-accepting CN groups on the imidazole moiety in solution, particularly for the parent fluorophore (Scheme 1). The efficiency of quenching decreases as the system becomes more extended and the energy of the singlet state decreases. There are at least two effects in these new probes under study (**1**–**6**) that might be responsible for the fact that the TEMPOL quenching for this series is not operative: i) the singlet energy of the probes is comparable to or lower than that of TEMPOL, and it was already indicated that fluorophores exhibit more effective ICT when the longest wavelength absorption band lies above 400 nm compared with the previous series; ii) there may be a steric effect from the large N,N-(dimethylaminophenyl) substituents in the C4/C5 positions of the imidazole moiety, which would weaken the paramagnetic effect of the free radical and increase the radiationless process in these fluorophores. Currently, it is difficult to determine which mechanism is operative.

The fluorescence lifetimes of the emissive state of the studied chromophores were experimentally determined in toluene and dichloromethane and ranged from 1.0 to 3.7 ns (Table 2). All decay curves were fitted by mono-exponential function. The most precisely determined lifetimes were those measured in toluene due to good signal. Rather narrow values ranged from 2.8 ns to 3.2 ns for all probes did not explain significantly structural differences of studied probes. The fluorescence lifetimes in polar solvents
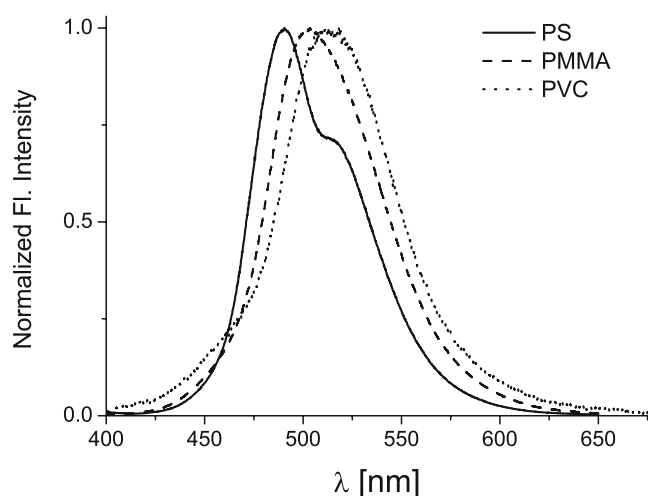
Fig. 9 Normalized emission spectra of **1** in polymer matrices at a concentration of 0.002 mol kg^{-1}. The excitation wavelengths were set at 398 nm in PS, 394 nm in PMMA and 389 nm in PVC

were not measured because of the low signal. The lifetimes were also estimated theoretically in the following manner. The fluorescence (radiative) rate constant (k_F) can be estimated

from the extinction coefficient (ε) (Table 1) using the following approximate relation [38].

$$k_{F-cal} = 10^4 \, \varepsilon \qquad (1)$$

The fluorescence lifetime can then be calculated as

$$\tau_{cal} = \Phi_F / k_{F-cal}. \qquad (2)$$

The longest lifetimes were observed in toluene and the highest fluorescence quantum yield was also observed in this solvent (Table 2). Interestingly, values were about 3 times lower in toluene and even one order lower in dichloromethane as those determined experimentally. Here as one of the possible explanations was that expressed radiative rate constant according to relation (1) did not match well the electron nature of the emissive state of push-pull molecule with strong charge-transfer absorption band. In polar solvents the estimated lifetime of the push-pull molecules under investigation was relatively short (1 to 500 ps) which correspond to low Φ_F of probes in such media. The fluorescence rate constants were lower up to one order of magnitude for polar

Table 4 Emission parameters of the investigated probes **1**–**6** in different polymer matrices

Probe[a]/Parameter	Medium[b]	λ_F[c] nm	Φ_F[d]	ν[e] cm^{-1}	τ[f] ns	k_{F-exp}[g] × 10^8 s^{-1}	k_{F-abs}[h] × 10^8 s^{-1}
1	PS	490, 522sh	0.69	4717	2.3	2.98	1.32
	PMMA	503	0.19	5500	1.9	1.00	2.63
	PVC	518	0.03	6402	2.2	0.11	2.00
2	PS	548	0.30	4847	2.6	1.16	1.58
	PMMA	559	0.16	5640	3.1	0.50	1.86
	PVC	554	0.06	5369	3.1	0.19	1.7
3	PS	584	0.09	5099	2.3	0.40	1.32
	PMMA	588	0.06	5669	2.2	0.29	1.78
	PVC	592	0.03	5991	2.1	0.13	1.58
4	PS	511	0.35	5493	2.5	1.39	1.62
	PMMA	518	0.13	6336	2.5	0.50	2.57
	PVC	522	0.05	6817	2.3	0.20	2.34
5	PS	543	0.21	5113	2.5	0.84	1.55
	PMMA	553	0.09	6307	2.9	0.30	2.19
	PVC	554	0.04	6280	2.9	0.12	2.45
6	PS	525	0.36	5224	2.5	1.44	1.51
	PMMA	538	0.10	6104	2.4	0.42	2.57
	PVC	538	0.06	6288	2.0	0.30	2.14

[a] Structure of probes **1**–**6** is according to Scheme 1

[b] Medium: PS—polystyrene; PMMA—poly(methyl methacrylate); PVC—poly(vinyl chloride)

[c] Maxima in emission spectrum ("sh" means shoulder). Excitation wavelength was set to the absorption maxima according to Table 1

[d] Quantum yield of fluorescence based on anthracene

[e] Stokes shift

[f] Lifetime of fluorescence. Decay was fitted to mono-exponential function

[g] Rate constant of fluorescence, k_{F-exp} calculated using experimental data of Φ_F and τ as ratio Φ_F/τ

[h] Rate constant of fluorescence, k_{F-abs} based on absorption spectra (Eq. 1)

solvent indicating that some specific quenching of the emissive state can occur.

Emission Characteristics in Polymer Matrices

The emission spectra of probes **2–6** in polymer matrices exhibited a wide un-structured band. The spectrum of probe **1** in non-polar PS exhibited a visible emission band at approximately 520 nm, which appeared as a shoulder to the main emission band (Fig. 9). The positions of the maxima depend on the π-linker nature; the most bathochromically shifted band was observed for probe **3** in a particular matrix similar to that observed in liquid media (Table 4). The fluorescence of the chromophores is more intense in commonly used polymer matrices compared with the intensities in polar and chlorinated solvents, and the highest intensity is observed in PS, ranging from 0.69 for **1** to 0.09 for **3** (Table 4). The quantum yields were comparable or only slightly lower than those of chromophores in the previous series of compounds. The fluorescence of these fluorophores is the most intense in PS; the fluorescence was approximately one order of magnitude lower in the chlorinated PVC matrix for all probes. The fluorescence intensity was relatively low in the PMMA matrix. The probes with the most conjugated π-linkers, such as planar probe **3** or the (*E*)-phenylethenylphenyl π-linker in **5**, exhibited the lowest Φ_F value of all the polymer matrices. It seems that such highly conjugated π–linkers support the formation of a non-emissive ICT state. The hindered rotations in a solid polymer matrix, which are responsible for the non-radiative dissipation of energy in low-viscosity liquid media, play a less important role. A similar trend was observed for chromophores **4–6**. The highest Φ_F value was determined for **6** (0.10 in PMMA, 0.36 in PS and 0.06 in PVC) with a fairly planar phenylethynyl-phenyl π-linker. The incorporation of a planar but more conjugated ethylene bridge between two 1,4-phenylene moieties in **5** resulted in a lower Φ_F value (0.09 in PMMA, 0.21 in PS and 0.04 in PVC). The shorter and more twisted biphenylene linker in **4** leads to the dissipation of energy, but this was not the case when the linker was incorporated into a solid polymer matrix. Probe **4** exhibited a higher Φ_F value than **5**, but this value was lower than that of **6**.

The Stokes shifts were relatively narrow for all probes in the particular polymer matrix (Table 4). However, these shifts nicely reflect the polarity of the matrix. Whereas in non-polar PS, the Stokes shifts lie within the range of 4700 to 5500 cm^{-1}, in relatively polar PMMA, these shifts lie within the range of 5500 to 6300 cm^{-1}. The largest Stokes shifts were observed in the PVC matrix (5400–6800 cm^{-1}, Fig. 9).

Since the fluorescence quantum yields were higher in polymer matrices as compared in solution the lifetimes of the probes **1–6** was determined in all matrices. The observed lifetimes lied in range from 1 to 3 ns (Table 4). Using experimentally determined values of $\Phi_{F\text{-exp}}$ and τ_{exp} in polymer matrices, the fluorescence rate constant was calculated as ratio of $\Phi_{F\text{-exp}}/\tau_{exp}$. The calculated fluorescence rate constants ($k_{F\text{-exp}}$) agreed well with those based on absorption spectra ($k_{F\text{-abs}}$) for low polar PS. On the other hand, these fluorescence rate constants were lower about one order of magnitude for PMMA and PVC indicating that some specific quenching of the emissive state occurred even in moderately polar polymer matrices.

1*H*-Imidazole derivatives with appended strong donating and accepting substituents and π-conjugated spacers are potentially applicable as materials for nonlinear optics (NLO). They are non-symmetric and exhibit (hyper)polarizability. In the series of compounds **1–6**, the π-conjugated system becomes more extended and, therefore, a bathochromic shift of the longest wavelength absorption band and an increased polarizability were observed. In polar media, in which the fluorescence is quenched, one might expect a higher degree of charge separation and a higher polarizability [39].

However, in polymer matrices with medium polarity such as PMMA or PVC, more intense fluorescence was observed, which implies a lower degree of charge separation and polarizability.

Conclusions

This study demonstrated that the new Y-shaped D-π–A systems featuring electron-donating substituents at the C4/C5 positions of the imidazole moiety yielded intense fluorescence in polymer matrices and non-polar solutions. The fluorescence intensities of the probes in non-polar toluene were comparable with those measured in polymer matrices. The extent of intramolecular charge-transfer in push-pull molecules based on 1*H*-methylimidazole in polar solvents should be studied using time-resolved spectrometry (laser flash photolysis). The position of the absorption and emission maxima can be finely tuned by the nature of the π-linker used. The length and planarity of the π-linker are the most important structural features affecting ICT in both series. However, the new series of imidazole-derived push-pull systems generally exhibited less intense fluorescence in all media than the previously studied derivatives based on imidazole-4,5-dicarbonitrile. Therefore, the previous imidazole-4,5-dicarbonitrile-based push-pull system [29] seems to be more suitable for photonics applications or sensor construction.

References

1. Jen AK-Y, Yue Zhang (1998) Electronoptic Polymers and Applications; Materials Based on Heteroaromatic Nonlinear optical Chromophores in Photonic Polymer Systems: Fundamentals, Methods and Applications, Eds.: Wise DL, Wnek GC, Trantolo DJ, Cooper TM, Gresser JD, Macel Dekker Inc. 270 Madison Avenue, New York, NY 10016–0602, Ch. 21 pp 847

2. Special issue on Organic Electronics and Optoelectronics, (2007), (Eds. S. R. Forrest, M. E. Thompson). Chem Rev 107:923–1386

3. Special issue on Materials for electronics, (2010), (Eds. R. D. Miller, E. A. Chandross), Chem Rev 110: 1–574

4. Special issue on Organic Photovoltaics, (2009), (Eds.: J. L. Brédas, J. R. Durrant), Acc Chem Res 42: 1689–1857

5. Grabowski ZM (1993) Electron transfer in flexible molecules and molecular ions. Pure Appl Chem 65:1751–1756. doi:10.1351/pac199365081751

6. Safarzadeh-Amiri A (1986) A time resolved fluorescence study of dynamic stokes shift of trans-4-dimethylamino-4′-cyanostilbene. Chem Phys Lett 125:272–278. doi:10.1016/0009-2614(86)87063-4

7. Abdel-Mottaleb MSA, Loufty RO, Laouyade R (1989) Non-radiative deactivation channels of molecular rotors. J Photochem Photobiol A 48:87–93. doi:10.1016/1010-6030(89)87093-5

8. Mqadmi S, Pollet A (1990) Non-radiative deactivation of p-(N, N-dialkylamino)- benzylidenemalonitriles. J Photochem Photobiol A 53:275–281. doi:10.1016/1010-6030(90)87131-T

9. Paczkowski J, Neckers DC (1991) The nature of the ground and excited states of substituted (N, N-dialkylamino)cinnamated and banzalmalonate. J Photochem Photobiol A 62:173–181. doi:10.1016/1010-6030(91)87018-Q

10. Wang SL, Ho TI (2000) Substituent effects on intramolecular charge-transfer behaviour of styrylheterocycles. J Photochem Photobiol A 135:119–126. doi:10.1016/S1010-6030(00)00289-6

11. Yesodha SK, Pillai ChKS, Tsutsumi N (2004) Stable polymeric materials for nonlinear optics: a review based on azobenzene systems. Prog Polym Sci 29:45–74. doi:10.1016/j.progpolymsci.2003.07.002

12. Bureš F, Schweizer WB, May JC, Boudon C, Gisselbrecht J-P, Gross M, Biaggio I, Diederich F (2007) Property tuning in charge transfer chromophores by systematic modulation of the spacer between donor and acceptor. Chem Eur J 13:5378–5387. doi:10.1002/chem.200601735

13. Wu YL, Bureš F, Jarowski PD, Schweizer WB, Boudon C, Gisselbrecht J-P, Diederich F (2010) Proaromacity: Organic charge–transfer chromophores with Smaal HOMO-LUMO gaps. Chem Eur J 16:9592–9605. doi:10.1002/chem.201001051

14. Bureš F, Schweizer WB, May JC, Boudon C, Gisselbrecht J-P, Gross M, Diederich F (2008) New push-pull chromophores featuring TCAQ (11,11,12,12-tetracyano-9,10-anthraquinodimethanes) and other dicyanovinyl acceptors. Eur J Org Chem 994–1004. doi:10.1002/ejoc.200700970

15. Bureš F, Pytela O, Diederich F (2009) Solvent effects on electronic absorption spectra of donor substituted 11,11,12,12-tetracyano-9,10-anthraquinodimethanes (TCAQs). J Phys Org Chem 22:155–162. doi:10.1002/poc.1443

16. Bureš F, Pytela O, Kivala M, Diederich F (2011) Solvatochromism as an efficient tool to study N, N-Dimethylamino- and Cyano-substituted π-conjugated molecules with an intramolecular charge-transfer absorption. J Phys Org Chem 24:274–281. doi:10.1002/poc.1744

17. Kulhánek J, Bureš F, Pytela O, Mikysek T, Ludvík J, Růžička A (2010) Push - pull molecules with a systematically extended π-conjugated system featuring 4,5-dicyanoimidazole. Dyes Pigm 85:57–65. doi:10.1016/j.dyepig.2009.10.004

18. Bureš F, Kulhánek J, Mikysek T, Ludwig J, Lokaj J (2010) Branched charge transfer chromophores featuring a 4,5-dicyanoimidazole unit. Tetrahedron Lett 51:2055–2058. doi:10.1016/j.tetlet.2010.02.067

19. Kulhánek J, Bureš F, Wojciechowski A, Makowska-Janusik M, Gondek E, Kityk VI (2010) Optical operation by chromophores featuring 4,5-dicyanoimidazole embedded within poly(methyl methacrylate) matrices. J Phys Chem A 114:9440–9446. doi:10.1021/jp1047634

20. Nepraš M, Almonasy N, Bureš F, Kulhánek J, Dvořák M, Michl M (2011) Fluorescence and photophysical properties of d-π-a systems featuring a 4,5-dicyanoimidazole unit. Dyes Pigm 91:466–473. doi:10.1016/j.dyepig.2011.03.025

21. Kulhánek J, Bureš F, Mikysek T, Ludvík J, Pytela O (2011) Imidazole as a central π-linkage in Y-shaped push - pull chromophores. Dyes Pigm 90:48–55. doi:10.1016/j.dyepig.2010.11.004

22. Kulhánek J, Bureš F, Pytela O, Mikysek T, Ludvík J (2011) Imidazole as a donor/acceptor unit in charge-transfer chromophores with extended π-linkers. Chem Asian J 6:1604–1612. doi:10.1002/asia.201100097

23. Plaquet A, Champagne B, Kulhánek J, Bureš F, Bogdan E, Castet F, Ducasse L, Rodriguez V (2011) Effects of the nature and length of the π-conjugated bridge on the second-order nonlinear optical responses of push-pull molecules including 4,5-dicyanoimidazole and its protonated forms. Chem Phys Chem 12:3245–3252. doi:10.1002/cphc.201100299

24. Jaing G, Michinobu T, Yuan W, Feng M, Wen Y, Du S, Gao H, Jiang L, Song Y, Diederich F, Zhu D (2005) Crystalline thin fims of s donor-substituted cyanoethene for nanoscale data recording through intramolecular charge-transfer interaction. Adv Mater 17:2170–2173. doi:10.1002/adma.200500559

25. Haldi A, Kimyonok A, Domercq B, Hayden LE, Jones SC, Marder SR, Weck M, Kippelen B (2008) Optimization of orange-emitting electrophosphorescent copolymers for organic light emitting diodes. Adv Funct Mater 18:3056–3062. doi:10.1002/adfm.200800446

26. Innocenzi P, Lebeau B (2005) Organic–inorganic hybrid materials for non-linear optics. J Mater Chem 15:3821–3831. doi:10.1039/b506028a

27. Cho MJ, Choi DH, Sullivan PA, Akelaitis APJ, Dalton LR (2008) Recent progress in second non-linear polymer and dendrimers. Prog Polym Sci 33:1013–1058. doi:10.1002/adma.200500559

28. Ma H, Lui S, Luo J, Sures S, Lui I, Kang SH, Haller M, Sassa T, Dalton LR, Jen AK-Y (2002) Highly efficient and thermally stable electro-optical polymers and dendrimers. Adv Funct Mater 12:565–574. doi:10.1002/1616-3028(20020916

29. Danko M, Hrdlovič P, Kulhánek J, Bureš F (2011) Push-pull fluorophores based on imidazole-4,5-dicarbonitrile: a comparison of spectral properties in solution and in polymer matrices. J Fluores 21:1779–1787. doi:10.1016/j.dyepig.2011.07.011

30. Birks JB (1968) Photophysics of Aromatic Molecules. Willey-Interscience a Division of John Wiley and Sons Ltd, New York, London, Toronto, Sidney, Ch 4 pp 121–127

31. Kawski A, Kubicki A, Kuklinski B, Gryczynski I (1993) Unusual absorption and fluorescence properties of 1,6-diphenyl-1,3,5-hexatriene in poly(vinyl alcohol) film. J Photochem Photobiol A 71:161–167. doi:10.1016/1010-6030(93)85068-J

32. Chorvat D Jr, Chorvatova A (2006) Spectrally resolved time-correlated single photon counting: a novel approach for characterization of endogenous fluorescence in isolated cardiac myocytes. Eur Biophys J 36:73–83. doi:10.1007/s00249-006-0104-4

33. Adamson AW, Demas JN (1971) Evaluation of photoluminescence lifetimes. J Phys Chem 57:2463

34. Demas JN (1973) Excited state lifetime measurements, Appendix E. Academic Press, New York, p 245

35. Enderlein J, Erdmann R (1997) Fast fitting of multi-exponential decay curves. Opt Commun 134:371–378, (http://www.joerg-enderlein.de/fluo/fluo.html)

36. Morimoto A, Yatsuhashi T, Shimada T, Biczók L, Tryk DA, Inoue H (2001) Radiationless deactivation of intramolecular charge transfer excited state through hydrogen bonding: effect of molecular structure and hard-soft anionic character in the excited state. J Phys Chem A 105:10488–10496. doi:10.1021/jp0117213

37. Danko M, Kosa C, Andics A, Vegh D, Hrdlovic P (2012) Spectral properties of chalcone containing triphenylamino structural unit in solution and in polymer matrices. Dyes Pigm 92:1257–1265. doi:10.1016/j.dyepig.2011.07.011

38. Bangar Raju B, Varadarajan TS (1995) Spectrosopic studies of 7-dimethylamino-3-styryl coumarins. J Photochem Photobiol A 85:263–267. doi:10.1016/1010-6030(94)03905-A

39. Hrobarik P, Sigmundova I, Zahradnik P, Kasak P, Arion V, Franz E, Clays K (2010) Molecular engineering of benzothiazolium salt with large quadratic hyperpolarizabilities: can auxiliary electron withdrawing groups enhance nonlinear optical response? J Phys Chem C 114:22289–22302. doi:10.1021/jp108623d